

## Reactivity assessment and spatial time-effects from the MUSE kinetics experiments

M. Carta<sup>\*1</sup>, A. D'Angelo<sup>1</sup>, V. Peluso<sup>1</sup>  
G. Aliberti<sup>2</sup>, G. Imel<sup>2</sup>, V. Kulik<sup>2</sup>, G. Palmiotti<sup>2</sup>  
J. F. Lebrat<sup>3</sup>, Y. Rugama<sup>3</sup>, C. Destouches<sup>3</sup>  
E. González-Romero<sup>4</sup>, D. Villamarín<sup>4</sup>  
S. Dulla<sup>5</sup>, F. Gabrielli<sup>5</sup>, P. Ravetto<sup>5</sup>  
M. Salvatores<sup>2,3</sup>

<sup>1</sup>ENEA, C.R. Casaccia, via Anguillarese, 301, 00060 S. Maria di Galeria, Rome, Italy

<sup>2</sup>Argonne National Laboratory, 9700 S. Cass Avenue, Argonne, Illinois, USA

<sup>3</sup>CEA, CEN Cadarache, 13108 St-Paul-lez-Durance, France

<sup>4</sup>CIEMAT, Avda. Complutense, 22, 28040, Madrid, Spain

<sup>5</sup>Politecnico di Torino, Corso Duca degli Abruzzi, 24, 10129, Torino, Italy

The MUSE program [1] is a series of zero-power experiments carried out at the CEA-Cadarache MASURCA facility since 1995 in the 5<sup>th</sup> European Framework, to study the neutronics of Accelerator Driven Systems (ADS). Among the main purposes of the MUSE experimental program there is the analysis of the possibility to infer the subcritical level of a source driven system using Pulse Neutron Source (PNS) methods, in view of the extrapolation of such methods to an European Transmutation Demonstrator (ETD). In this paper, the MUSE results obtained on a significantly subcritical MUSE-4 configuration are analyzed on the basis of both theoretical backgrounds and corresponding calculation simulations.

**KEYWORDS: Reactivity Measurements, MUSE, ETD, ADS**

### 1. Introduction

In order to detect any unexpected reactivity variation and allow the continuous check of the sub-criticality margin during the operation, the absolutely calibrated subcriticality level will need to be continuously monitored in Accelerator Driven Systems (ADS) and in particular in the European Transmutation Demonstrator (EDT). This subcriticality level monitoring will also allow the check between experimental and foreseen fuel cycle and temperature variations reactivity effect.

Among the main purposes of the MUSE experimental program [1], that is being carried out in the zero-power MASURCA European facility, there is the analysis of the possibility to infer the subcritical level of a source driven system using Pulse Neutron Source (PNS) methods [2, 3, 4], in view of the extrapolation of such methods to an European Transmutation Demonstrator (EDT). In this aim, one of the MUSE-4 phase objectives is the investigation of the system response to neutron pulses, provided by the GENEPI pulsed deuteron accelerator, with frequencies from 50 Hz to 4.5 kHz, and less than 1 $\mu$ s wide, generated at the reactor center by (d, d) and (d, t) reactions. Detectors

---

\* Corresponding author, Tel. +39-06-3048-3183, FAX +39-06-3048-6308, E-mail: carta@casaccia.enea.it

mainly based on  $^{235}\text{U}$  fission, located in the core, reflector and shielding regions, are used for measuring the time dependent responses.

In this paper, the results obtained for a MUSE-4 configuration characterized by a low subcritical level (about -12 \$) have been analyzed on the basis of both theoretical backgrounds and corresponding calculation simulations. In particular, both PNS area and  $\alpha$ -fitting classical methods for measuring the subcriticality level have been analyzed, giving indications about the performance of such methods when applied to the MUSE case.

## 2. Theoretical Background

### 2.1 General Considerations

As well known, all the methods applied to infer the criticality level of a given neutron multiplicative system are based on point kinetics assumption. Depending on both the distance from criticality and the arise of time-dependent transport effects, the point kinetics approach may require more or less pronounced "correction" factors, determined by calculations, to actually infer the subcritical level by detector responses in given positions in the system. Consequently, we can assume that a certain method for a given system is more or less reliable on the basis of the order of magnitude of such corrections factors.

Such considerations are valid also for the source jerk method, not taken into account in this report because not applied for the selected MUSE-4 configuration. It should be mentioned that the MUSE-4 experiment, because the pulsed regime of the external source, together with the characteristics (frequency, pulse duration) of the GENEPI accelerator, does not allow for an "explicit" application of the source jerk method. The possibility to apply "equivalent" source jerk methods is still under discussion.

As previously mentioned, we will analyze the experimental results relative to the two PNS experimental methods (area and  $\alpha$ -fitting) applied for the MUSE-4 configuration under discussion.

For what concerns the PNS  $\alpha$ -fitting method it is possible, when looking at experimental data, to foresee "a priori" three classes of possible MUSE-4 responses to a short pulse:

a) The system responses exhibit the same  $1/\tau$ -slope for all the positions (core, reflector, and shield). The system seems to act as a point, and point kinetics seems to be applicable without correction factors.

b) For a given position (core, reflector, shield), the system response exhibits a  $1/\tau$ -slope, but such slopes are different if compared one each other. Thus, at least a "local" point kinetics behavior is observed:  $\alpha$ -fitting methods, which invoke for an estimate of the neutron mean generation time  $\Lambda$ , will provide reactivity values (in dollars) apparently depending on the detector position. Correction factors are required.

c) The system responses do not exhibit  $1/\tau$ -slopes: only fitting procedures on the experimental data can try to smooth the problem, in the effort to reproduce, if possible, situations similar to case b). Correction factors are required.

On the contrary, for what concerns PNS area methods (which do not invoke for estimates of  $\Lambda$ ), it is not possible "a priori" to estimate the need or less of correction factors even if the system response appears to be different from a point kinetics behavior. This aspect is strictly connected with the integral nature of the PNS area methods.

## 2.2 PNS $\alpha$ -fitting method

PNS  $\alpha$ -fitting method requires an accurate evaluation of the "expected"  $\alpha_p$ , and of the associated neutron mean generation time  $\Lambda$ , to take into account kinetics distortion effects resulting in different flux shapes respect to those predicted by eigenvalue calculations. In particular, assuming the complete time separability of the flux into an amplitude function and a shape function:

$$\phi(\mathbf{r}, E, \boldsymbol{\Omega}, t) = P(t)\psi(\mathbf{r}, E, \boldsymbol{\Omega})$$

and, consequently, assuming that the system responses exhibit the same  $\alpha$ -slope:

$$P(t) = P_0 e^{\alpha_p t}$$

it is easily demonstrated that the shape function  $\psi(\mathbf{r}, E, \boldsymbol{\Omega})$  is the eigenfunction of the following  $\alpha_p$ -eigenvalue equation in the prompt-time domain:

$$\boldsymbol{\Omega} \cdot \nabla \psi + \left[ \Sigma_t \psi + \frac{\alpha_p}{v} \psi \right] = \langle \Sigma_{\text{ins}} \psi \rangle + (1 - \beta) \chi_p \langle v \Sigma_f \psi \rangle$$

Once the shape function and the  $\alpha_p$ -eigenvalue are obtained, the neutron mean generation time  $\Lambda$  can be evaluated as:

$$\Lambda = \frac{\langle \phi^* \frac{1}{v} \psi \rangle}{\langle \phi^* \chi_p \langle v \Sigma_f \psi \rangle \rangle}$$

and taking into account that  $\beta$  is the average delayed neutron fraction over the different fuel zones, the reactivity is obtained accordingly to the prompt version of the inhour equation:

$$\rho = \alpha_p \Lambda + \beta$$

## 2.3 Area Method

The area method [3] is based on the following relationship relative to the areas subtended by the system responses to a neutron pulse:

$$\frac{-\rho}{\beta_{\text{eff}}} = \frac{\text{prompt neutron area}}{\text{delayed neutron area}} \equiv \frac{I_p}{I_d}$$

Because of spatial effects, the reactivities are functions of detector position. As shown in [4], these spatial effects can be taken into account. Supposing that the neutron source is represented by:

$$Q(\mathbf{r}, E, \boldsymbol{\Omega}, t) = Q(\mathbf{r}, E, \boldsymbol{\Omega}) \delta_+(t)$$

the time integrated prompt-neutron flux satisfy the ordinary time-independent (static) transport equation. Therefore the spatial effect due to the harmonics (switched on by the external source) can be taken into account by means of two time-independent calculations solving the complete and the following “prompt-neutron-only” inhomogeneous (with source) transport equations relevant to the considered system (and source distribution):

$$\mathbf{\Omega} \cdot \nabla \tilde{\Phi}_p + \Sigma_t \tilde{\Phi}_p = \langle \Sigma_{\text{in scat}} \tilde{\Phi}_p \rangle + (1-\beta)\chi_p \langle \nu \Sigma_f \tilde{\Phi}_p \rangle + Q(\mathbf{r}, E, \mathbf{\Omega})$$

with:

$$\tilde{\Phi}_p \equiv \int_0^{\infty} \Phi_p(\mathbf{r}, E, \mathbf{\Omega}, t) dt$$

The spatial dependence of the area method is function of detector position,  $\mathbf{R}$ , through the spatial dependence of  $\sigma_{\text{detector}}$ :

$$\frac{I_p(\mathbf{R})}{I_d(\mathbf{R})} = \frac{\iiint \sigma_{\text{de tector}}(\mathbf{r} - \mathbf{R}, E) \tilde{\Phi}_p dV dE d\mathbf{\Omega}}{\iiint \sigma_{\text{de tector}}(\mathbf{r} - \mathbf{R}, E) (\tilde{\Phi} - \tilde{\Phi}_p) dV dE d\mathbf{\Omega}}$$

### 3. Pre-Analysis

#### 3.1 $\Lambda$ and $\alpha_p$ dependence on subcriticality

The calculation strategy recently proposed in [5] was used to solve the  $\alpha_p$ -eigenvalue equation by the ERANOS [6] code system by solving a K-eigenvalue equation type. The  $\alpha_p$ -eigenvalue problem was solved by an additional absorption term  $\alpha/v$  ( $v$  neutron velocity), assuming the prompt neutron spectrum, and searching for the  $\alpha_p$ -eigenvalue giving  $K_{\text{eff}} = 1$ .

Successively, it was evaluated the impact on the point kinetics parameters by using the above "rigorous" point approach respect to the approximated one, based on the solution of the k-eigenvalue equation:

$$\mathbf{\Omega} \cdot \nabla \Phi_k + \Sigma_t \Phi_k = \langle \Sigma_{\text{in scat}} \Phi_k \rangle + \frac{\chi(E)}{K} \langle \nu \Sigma_f \Phi_k \rangle$$

and deriving the point kinetics parameters as (subscript k indicates relative to k-eigenvalue equation):

$$\alpha_{p,k} = \frac{\rho_k - \beta_{\text{eff}}}{\Lambda_k}; \quad \rho_k = \frac{K-1}{K}$$

$$\beta_{\text{eff}} = \frac{\sum_i \beta_i \langle \Phi^* \chi_i \langle \nu \Sigma_f \Phi_k \rangle \rangle}{\langle \Phi^* \chi \langle \nu \Sigma_f \Phi_k \rangle \rangle}; \quad \Lambda_k = \frac{\langle \Phi^* \frac{1}{v} \Phi_k \rangle}{\langle \Phi^* \chi \langle \nu \Sigma_f \Phi_k \rangle \rangle}$$

As first step, the subcritical MUSE-4 976 cells core configuration (in the frame of the calculation benchmark launched by CEA [7]) was considered, and a preliminary analysis was performed by means of the CEA ERANOS deterministic codes system in conjunction with JEF2.2 data.

A RZ model was assessed (Fig. 1), the symmetry axis being around the GENEPI pulsed-accelerator beam pipe axis. To perform cross sections processing, a macro-cell calculation was carried out by means of ERANOS ECCO cell code [8]; 50 energy groups cross sections were obtained by a fine energy group structure collapsing, and RZ transport calculations were performed by means of BISTRO spatial module [9].

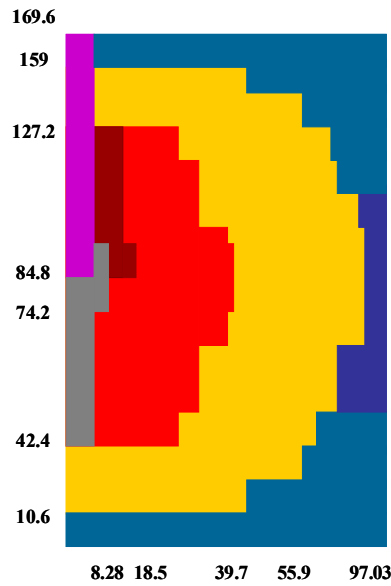


Fig. 1 X-Y and RZ view of the 976 cells configuration for the MUSE-4 pre-analysis.

The "approximated"  $\alpha_{p,k}$  and the "rigorous"  $\alpha_p$  calculation procedures were performed assuming different reactivity levels (assessed by varying the core radius in the RZ subcritical configuration); results are shown in Tab. 1 where green bold data indicate the values directly calculated by ERANOS code system and red bold ones indicate derived values.

Table 1 Comparison between the point kinetics parameters coming from  $k$  and  $\alpha_p$  eigenvalue calculation at different subcritical reactivity levels.

	$K_{\text{eff}}$	$\rho$ (pcm)	$\beta_{\text{eff}}$ (pcm)	$\Lambda_k$ ( $\mu\text{s}$ )	$\alpha_{p,k}$ ( $\text{s}^{-1}$ )
k eigenvalue calculation	0.97124	<b>-2961</b>	335	0.5163	<b>-63834</b>
	0.99140	<b>-867</b>	334	0.4981	<b>-24121</b>
	1.00729	<b>724</b>	<b>335</b>	0.4823	<b>8059</b>
	1.02647	<b>2579</b>	333	0.4644	<b>48357</b>
	$K_d$	$\rho$ (pcm)	$\beta$ (pcm)	$\Lambda$ ( $\mu\text{s}$ )	$\alpha_p$ ( $\text{s}^{-1}$ )
$\alpha_p$ eigenvalue calculation	0.97166	<b>-2916</b>	369	0.8163	<b>-40240</b>
	0.99128	<b>-879</b>	371	0.5556	<b>-22500</b>
	1.00723	<b>717</b>	373	0.4714	<b>7300</b>
	1.02640	<b>2572</b>	377	0.4142	<b>53000</b>

Results show that:

- The ratio  $\alpha_p/\alpha_{p,k}$  deviates from unit depending on the subcritical system reactivity level. In Fig. 2 are shown the  $\alpha_p/\alpha_{p,k}$  ratio values relative to the results in Tab. 1;

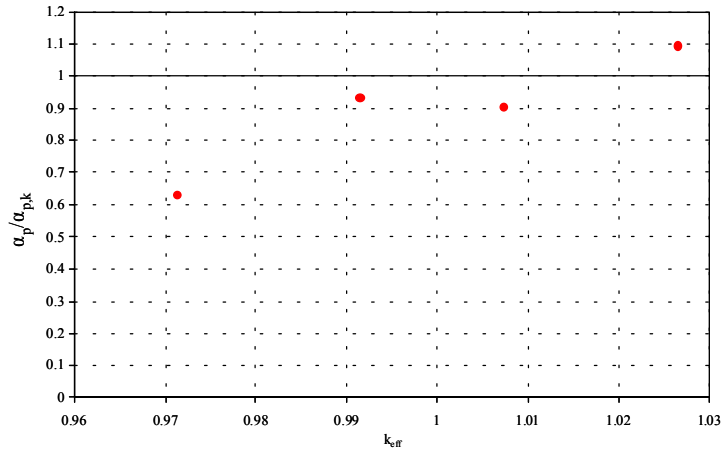


Fig. 2  $\alpha_p/\alpha_{p,k}$  ratio at different reactivity levels.

- Far from criticality, the differences between  $\alpha_p$  and  $\alpha_{p,k}$  are mainly due to the differences between the mean neutron generation times  $\Lambda$  evaluated using  $\Phi_k$  or  $\psi$  eigenfunctions;
- Differences between reactivity evaluated using  $\Phi_k$  or  $\psi$  eigenfunctions are less important, due to the large compensations in the product  $\alpha \cdot \Lambda$  relative to the dynamic reactivity;
- Differences between  $\psi$  and  $\Phi_k$  eigenfunctions energy profiles are found, mainly, in the reflector and shield zones at low energies (Fig. 3).

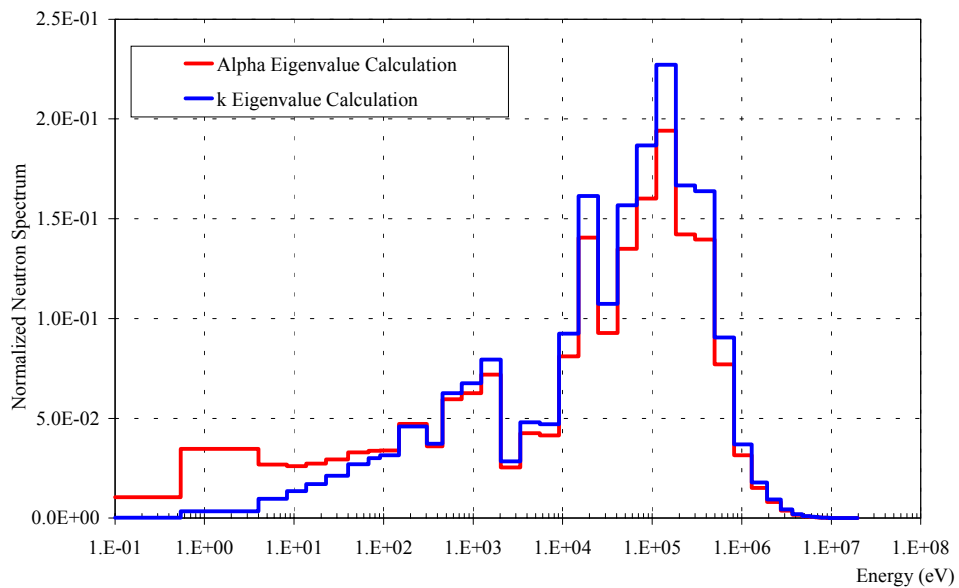


Fig. 3  $\psi$  (red line) and  $\Phi_k$  (blue line) eigenfunctions neutron spectra in a detector position in the reflector.

Finally, this preliminary investigation showed that only the kinetics parameters obtained by "rigorous"  $\alpha_p$  calculation procedures can be used to correctly analyze  $\alpha_p$ -slope experimental results. This need is pointed out by the large discrepancy existing between the refined  $\Lambda$  and the approximated  $\Lambda_k$  results of Tab. 1 and is confirmed by the evident neutron spectrum distortion induced by the K-eigenvalue approximation shown in Fig. 3.

### 3.2 Area Method

A preliminary investigation of the area method response dependence on the detector position is carried out by time-dependent, one energy group analytical calculations on a reflected core having 1D slab geometry. Core and reflector compositions are representative of the MUSE case. The system is characterized by the following parameters:

$$\begin{aligned}\beta &= 335 \text{ pcm} \\ \lambda &= 0.084 \text{ s}^{-1} \\ \Lambda &= 0.586 \text{ } \mu\text{s} \\ \rho &= -4200 \text{ pcm}\end{aligned}$$

A Dirac delta-function representation is assumed for neutron pulses having a period T:

$$S(x, t) = \sum_{i=0}^I \delta(x) \delta(t - iT)$$

and the following flux integrals were used to evaluate factors proportional to the prompt and delayed detector responses:

$$\begin{aligned}I_{\text{tot}}(x) &= \int_T \Phi(x, t) dt \\ I_d(x) &= \Phi(x, T) \cdot T \\ I_p(x) &= I_{\text{tot}}(x) - I_d(x)\end{aligned}$$

Fig. 4 shows the area method ratio  $I_p/I_d$  in function of the detector position. The same ratio is represented as normalized to the expected  $\rho/\beta$  value. Dotted line represents  $I_p/I_d$  mean value.

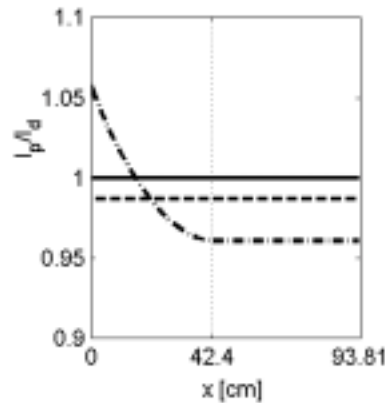


Fig. 4 Prompt and delayed area ratio versus the detector position.

It can be seen that, in the case of a MUSE-like reflected reactor, the predicted spatial dependence of the area method remains limited within 6% of its average value (dotted line), and that this average value is well close to unity.

The encouraging results of this area method preliminary analysis will be checked in the following when analyzing the MUSE experimental results (see paragraph 4.3). The effects of the detector position will be evaluated taking into account the energy dependence of the responses and the actual geometry of the system (GENEPI accelerator, core, control rods, shield, reflector).

## 4 Analysis of the Experimental Results

### 4.1 Configuration SC0 DT / 1108 cells

Experimental results relevant to the MUSE-4 SC0 1108 fuel cells configuration with a D-T external source ( $3.3 \cdot 10^6$  n/pulse of 14 MeV) located in the reactor center (Fig. 5) have been analyzed in this paper. The configuration having 3 Safety Rods (SR) up, SR1 down and Pilot Rod (PR) down is characterized by a significant subcriticality (about  $-12.5 \%$ ), by a large availability of experimental results measured at a such subcriticality level [10, 11], and by statistics of the time-depending experimental results that are clearly better than those reachable with a D-D external source.

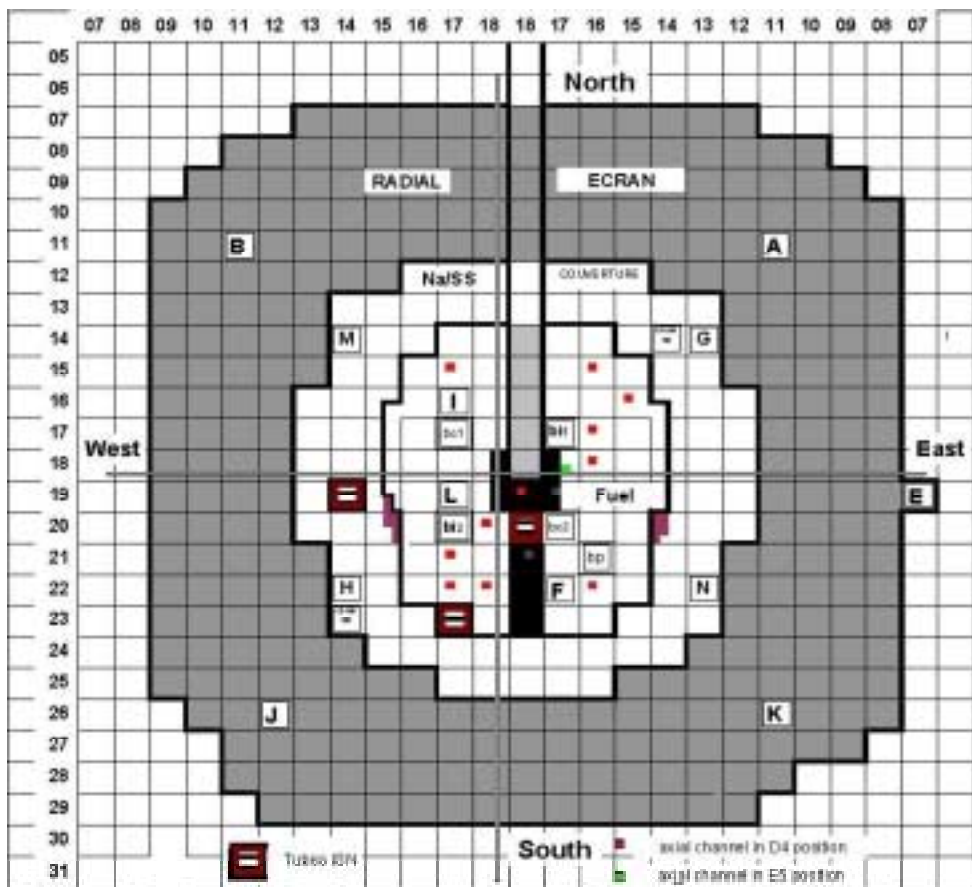


Fig. 5 XY view of MUSE-4 SC0 1108 cells configuration.

Moreover, in a previous campaign of measurements using D-D source, carried out by the MASURCA team on a MUSE-4 SC0 1086 fuel cells configuration very close to the 1108 fuel cells configuration of the case with D-T external source, the MSM subcriticality level was also measured. The MSM experimental results with PR down and with 3 SR up, and SR1 and PR down, were respectively  $-1.74 \$$  and  $-12.53 \$$  ( $\beta_{\text{eff}}=335$  pcm) [10]. Owing to the difference of only 0.2 \$ between the two configurations with PR down (the DT configuration subcriticality level with only the pilot rod down was  $-1.95 \$$  [10]), the reactivity measured by MSM in the SC0 1086 cells ( $-12.53 \$$ ,  $\approx -4200$  pcm) was assumed as reference reactivity level also for the SC0 1108 cells configuration considered in this paper.

#### 4.2 Slope Analysis by $\alpha$ -fitting Method

A XY model was assessed and 33 energy groups transport calculations were performed by means of ERANOS deterministic code system using BISTRO spatial module.

The procedures described in 3.1 were performed, results being shown in Tab. 2 (as above, green bold data indicate the values directly calculated by ERANOS code system and red bold ones indicate derived values).

Table 2 Comparison among point kinetics parameters coming from k and  $\alpha_p$  eigenvalue calculation.

	$K_{\text{eff}}$	$\rho$ (pcm)	$\beta_{\text{eff}}$ (pcm)	$\Lambda_k$ ( $\mu\text{s}$ )	$\alpha_{p,k}$ ( $\text{s}^{-1}$ )
k eigenvalue calculation	0.95970	<b>-4200</b>	335	0.4683	<b>-96821</b>
	$K_d$	$\rho$ (pcm)	$\beta$ (pcm)	$\Lambda$ ( $\mu\text{s}$ )	$\alpha_p$ ( $\text{s}^{-1}$ )
$\alpha_p$ eigenvalue calculation	0.95843	<b>-4337</b>	368	1.0069	<b>-46730</b>

It can be noted the large compensation in the product  $\alpha_p \cdot \Lambda$ , as the preliminary investigation showed too: passing from the  $\alpha_p$  eigenvalue calculation to the k eigenvalue calculation, while  $\alpha_p$  value is doubled,  $\Lambda$  is halved. Moreover, dynamic simulations were performed by means of either the ERANOS codes system (KIN3D model in conjunction with JEF2.2 library) [12] or by the MCNP code [13] (ENDF/B-VI library was used). KIN3D, that solves direct (without any point-approximation) spatial XYZ kinetics, has been used for 33 energy groups calculations.

The  $^{235}\text{U}$  fission detectors responses in three different positions in the reactor were calculated; Fig. 6 shows the results obtained by means of the  $\alpha_p$  eigenvalue investigation, the ERANOS KIN3D module and the MCNP code.

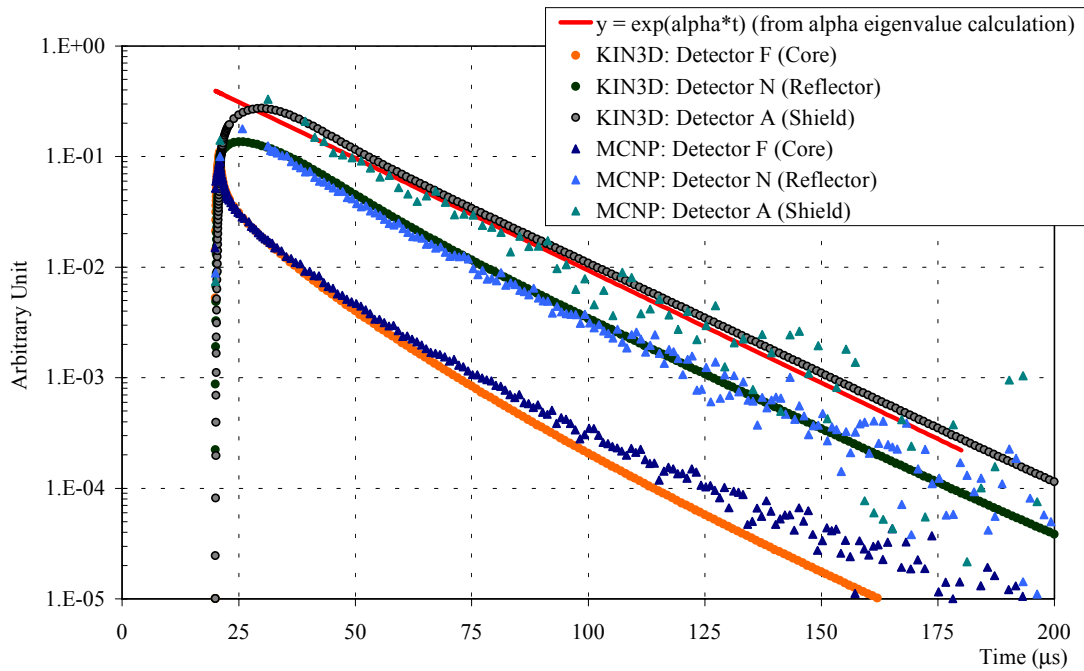


Fig. 6  $^{235}\text{U}$  responses calculated by KIN3D, MCNP and  $\alpha$  eigenvalue procedure.

Time-dependent (KIN3D and MCNP) calculation results seem to provide a coherent picture concerning the system location where PNS  $\alpha$  method (with refined  $\Lambda$  evaluation) could be applied, i.e. far from the source. In any case, point kinetics  $\alpha_p$  slope seems to agree with exponential  $1/\tau$ -slope only in the shield and for a short time period. In Fig. 7, MCNP calculation results have been compared with the experimental shapes in the same positions.

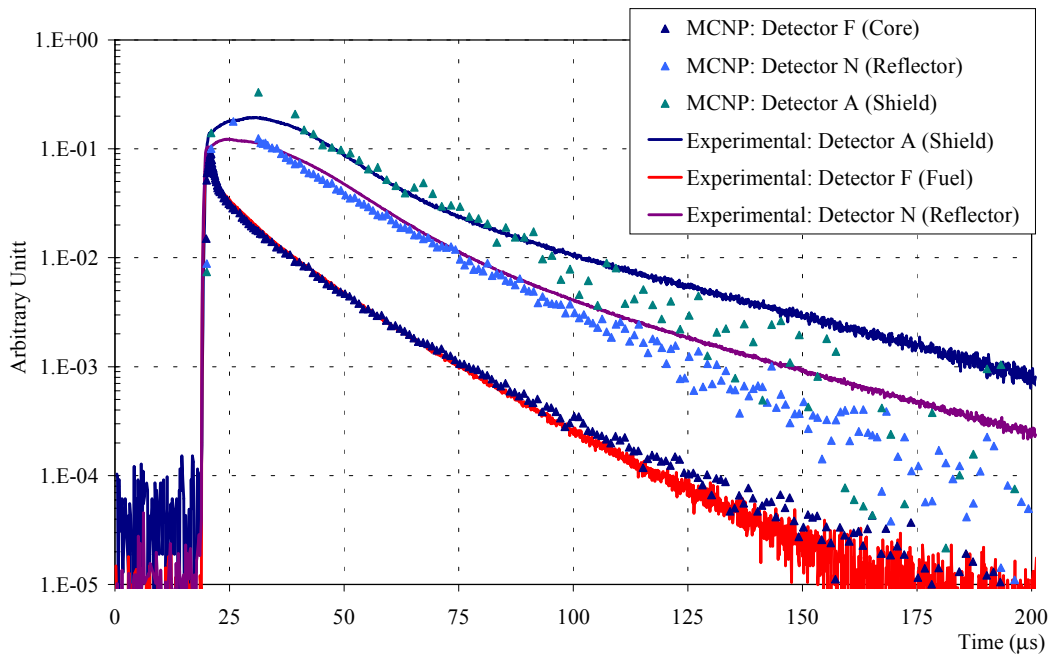


Fig. 7 Comparison between experimental and MCNP calculated  $^{235}\text{U}$  responses.

Experimental results show that for large subcriticalities,  $1/\tau$ -slopes are different for core, reflector and shield detectors positions. MCNP results well reproduce in the core the experimental responses. Moreover, reflector and shield experimental slopes show a double exponential behavior which is not reproduced by MCNP calculations; on the contrary, it looks evident a good agreement for a short time period.

Finally, point kinetics  $\alpha_p$  slope seems to agree with experimental slopes only in the shield, and for a short time period.

### 4.3 Area Method Analysis

The spatial dependence of the area method results has been calculated using the static approach described above (par. 2.3), by means of ERANOS deterministic codes system with the XY geometry and 33 energy groups cross sections used for  $\alpha_p$  eigenvalue calculation.

Two inhomogeneous BISTRO transport calculations with the D-T external source were performed assuming the total fission spectrum  $\chi$  and the prompt fission spectrum  $\chi_p(1-\beta)$ : as result the flux  $\Phi$  and the prompt flux  $\Phi_p$  were obtained.

In each  $^{235}\text{U}$  detectors position (see Fig. 5), the following quantities were calculated:

- The total area, i.e. the  $^{235}\text{U}$  fission rate using the flux  $\Phi$ ;
- The prompt area, i.e. the  $^{235}\text{U}$  fission rate using the flux  $\Phi_p$ ;
- The delayed area, by subtracting the prompt area from the total one;
- The reactivity (in dollars), by dividing the prompt and the delayed area.

Results have been compared with the experimental values [11] in Tab. 3, where the ratio between each value in each detector position and the reference reactivity level ( $\rho = -12.53$  \$) is also shown in the “dispersion” column.

Table 3 Reactivity evaluation by means of PNS area method: comparison between the experimental and calculated values.

Detector	Reactivity (\$)		Dispersion		
	Exp.	Cal.	Exp.	Cal.	(E-C)/C (%)
I	-14.3	-13.1	1.14	1.06	+7.5
L	-12.9	-13.0	1.03	1.03	-0.6
F	-11.9	-11.8	0.95	0.94	+0.7
M	-12.7	-12.8	1.01	1.02	-0.8
G	-13.0	-12.4	1.04	0.99	+5.0
N	-12.1	-11.8	0.96	0.94	+2.2
H	-12.6	-12.1	1.00	0.96	+4.3
A	-12.7	-12.4	1.01	0.98	+2.8
B	-13.0	-12.8	1.04	1.01	+1.9

Tab. 3 shows a good agreement among the calculated values and the experimental results. Only the highest reactivity result relevant to the detector I, very close to the SR1 control rod (see Fig. 5), is not completely reproduced by the calculation.

In any case, our investigation indicates that PNS area method seems to be more reliable (spatial correction factors about  $\pm 5\%$ ) respect to PNS  $\alpha$ -method. In general, this evident consideration can be connected with the previously mentioned integral nature of the PNS area methods, which do not invoke for estimates of  $\Lambda$ . In particular, we have verified that the spatial dependence of the area method can be evaluated by steady state calculations allowing taking into account of the harmonics switched on by the external source [4].

## 5 Conclusions

The PNS-methods experimental results relative to the MUSE-4, SC0, 1108 fuel cells, D-T source configuration with 3 SR up, SR1 down and PR down have been analyzed. Both the area and the  $\alpha$ -fitting methods have been simulated by different methods and codes: CEA ERANOS code system in conjunction with JEF2.2 data for static calculations devoted to the evaluation of point kinetic parameters and of the spatial dependence relevant to the area method; spatial time-dependent calculations by direct solutions of the 3D kinetic module KIN3D; Monte Carlo spatial time-dependent simulations in conjunction with ENDF/B-V data. The analysis of the experimental results gives the following indications, either on the PNS methods performance when applied to the MUSE case or, more in general, on their application to the ETD situation:

1. For large subcriticalities, only PNS area method seems to be reliable for what concerns the order of magnitude of the spatial correction factors (about  $\pm 5\%$ ). Concerning its application to the ETD situation, considering the beam time structure required for an ETD, it does not allow an on-line subcritical level monitoring, but can be used as "calibration" technique with regards to some selected positions in the system to be analyzed by alternative methods, like Source Jerk/Prompt Jump (which can work also on-line).
2. Codes and data are capable to predict the MUSE time dependent behavior in the core region. The presence of a second exponential behavior in the reflector and shield zones is not evidenced either by the deterministic or by the Monte Carlo simulations. More statistics in Monte Carlo analysis seems to be required to predict "late" transport phenomena, even if such phenomena are not explicitly correlated to the subcritical level.
3. As mentioned before, MUSE-4 experiment, because of the characteristics of the GENEPI accelerator, does not allow for an "explicit" application of the source jerk method. The possibility to apply "equivalent" source jerk methods is still under discussion. In this aim TRADE experiment, where an external spallation neutron steady source is foreseen, can help to clarify the role of such technique for on-line monitoring of the subcritical level of future ETD.

## REFERENCES

- 1) M. Salvatores et al., "MUSE-1: A First Experiment at MASURCA to Validate the Physics of Sub-Critical Multiplying Systems Relevant to ADS", Proc 2nd Int Conf on Accelerator-Driven Transmutation Technologies and Applications, Kalmar, Sweden, Vol 1, p 513, 1996.
- 2) B.E. Simmons and J.S King: "A Pulsed Neutron Technique for Reactivity Determination", Nucl. Sc. and Eng., 3, 595 (1958).
- 3) N.J. Sjöstrand, Arkiv. Fis. 11, 233 (1956), see also in G.I. Bell and S. Glasstone, "Nuclear Reactor Theory", (pp.546-549), 1970, Van Nostrand Reinhold Company.
- 4) E. Garelis and J. Russel, Nucl. Sc. and Eng., 6, 263 (1963), see also in G.I. Bell and S. Glasstone, "Nuclear Reactor Theory", (pp.550), ibidem.
- 5) J.E. Hoogenboom, "Numerical Calculation of the Delayed-a Eigenvalue using a Standard Criticality Code", Proc. PHYSOR 2002, Seoul, Korea, October 7-10, 2002.
- 6) G. Rimpault et al., "The ERANOS code and data system for fast reactor neutronic analyses", Proc. PHYSOR 2002, Seoul, Korea, October 7-10, 2002.
- 7) E. González-Romero, R. Soule, D. Villamarin, "Benchmark on Computer Simulation of MASURCA critical and subcritical experiments (MUSE-4 benchmark)", NEA/SEN/NSC/WPPT(2001)5, For Official Use.
- 8) G. Rimpault, "Algorithmic Features of the ECCO Cell Code for Treating heterogeneous Reactor Subassemblies", Int. Conf. On Mathematics and Computations, Reactor Physics and Environmental Analyses, Portland, OR, April 30 – May 4, 1995.
- 9) G. Palmiotti, J. M. Rieunier, C. Gho, M. Salvatores, "BISTRO Optimized Two Dimensional Sn Transport Code", Nucl. Sc. and Eng., 104, 26 (1990).
- 10) F. Mellier, Personal Communication.
- 11) E. González-Romero et al., "Pulsed neutron source measurements of kinetic parameters in the source-driven fast subcritical core MASURCA", Proc. of the International Workshop on P&T and ADS Development, organized on behalf of the "ADvanced Option for Partitioning & Transmutation Thematic Network (ADOPT), SCK-CEN, Mol, Belgium, October 6-8, 2003.
- 12) A. Rineiski, W. Maschek, G. Rimpault, "Performance of Neutron Kinetics Models for ADS Transient Analyses", AccAPP/ADTTA'01, ANS 2001 Winter Meeting, Reno, Nevada (USA), November 11-15, 2001.
- 13) J. F. Briesmeister (Editor), "MCNP4C – A General Monte Carlo Code N-Particle Transport Code", Los Alamos National Lab., LA-13709-M (2000).